# KINEMATIC CHARACTERISTICS ANALYSIS AND TEST OF DOUBLE-ROW VIBRATING CASSAVA HARVESTER

双行振动式木薯收获机运动学特性分析与试验

Guanghao XU<sup>1)</sup>, Jiannong SONG<sup>2)</sup>, Zhongsheng CAO<sup>1)</sup>, Binfeng SUN<sup>1)</sup>, Junbao HUANG<sup>1)</sup>, Xinyi PENG<sup>1)</sup>, Wenwen LI<sup>1,3)</sup>, Yanda LI<sup>1\*)</sup>

<sup>1)</sup> Institute of Agricultural Engineering, Jiangxi Academy of Agricultural Sciences, Nanchang 330200 / China;
<sup>2)</sup> College of Engineering, China Agricultural University, Beijing 100083 / China
<sup>3)</sup> College of Engineering, Jiangxi Agricultural University, Nanchang; 330045 / China
\* Corresponding author: Yanda LI
Tel: +86-15870656983; E-mail: liyanda2008@126.com

DOI: https://doi.org/10.35633/inmateh-77-74

Keywords: cassava, vibration harvester, motion analysis, field experiment

### **ABSTRACT**

To address the low level of standardization in cassava planting and the poor operational performance of existing harvesting machinery in China, this study proposes a wide-ridge, double-row cassava planting pattern that integrates current agronomic practices with harvesting requirements. Based on this planting pattern, a double-row vibrating cassava harvester was designed, and its overall structure and key parameters were determined. Using analytical methods, the displacement equation and motion-trajectory equation of the digging-shovel tip were established, and the corresponding motion-trajectory plots were generated using MATLAB. The cutting, lifting, and impact interactions between the digging shovel and the soil/cassava—soil complex were theoretically analyzed. Field tests of the prototype showed that its pure working productivity reached  $\geq 0.52 \text{ hm}^2\text{/h}$ , the clean-root rate was  $\geq 97.33\%$ , the damaged-root rate was  $\leq 1.43\%$ , and the total loss rate was  $\leq 2.67\%$ . The results demonstrate that the double-row vibrating cassava harvester operates stably and reliably. The vibrating digging shovel exhibits strong soil-breaking ability and enables rapid and effective separation of cassava from the soil. All performance indicators meet or exceed the design specifications.

#### 摘要

针对中国木薯种植标准化程度低、现有收获机械作业性能差等问题,本研究结合现有木薯种植农艺和收获要求,制定了大垄双行木薯种植模式,依据此模式设计了双行振动式木薯收获机,确定了整机结构及主要技术参数。通过解析法建立了挖掘铲铲尖角位移方程和运动轨迹方程,借助用 MATLAB 软件获取了铲尖的运动轨迹图像,并从理论上分析了挖掘铲对土壤及薯土复合体之间的切削、抬升和撞击的作业机理。进行了样机田间试验,得到样机纯工作小时生产率  $\geq 0.52 \text{ hm}^2/\text{h}$ 、明薯率  $\geq 97.33\%$ 、伤薯率  $\leq 1.43\%$ 、总损失率  $\leq 2.67\%$ 。试验结果表明,双行振动式木薯收获机工作稳定可靠,振动挖掘铲碎土效果好,薯土分离迅速、彻底,各项性能指标均达到或优于设计要求。

## INTRODUCTION

Cassava, originated from Brazil, is one of the main edible and feeding plants in the world. It is also a typical food crop in tropical and subtropical poverty-stricken areas. It is listed as the world's three largest potato crops together with potato and sweet potato (*Ferraro et al., 2016*; *He et al., 2020*; *Otun et al., 2023*). Cassava is widely planted in tropical and subtropical areas, and was introduced to coastal provinces and cities in southern China in the early 19th century (*Tan et al., 2018*). Cassava harvesting is the most intensive and laboroccupied process in cassava production, accounting for 61% of the whole cassava production (*Huang et al., 2012*). With the increase of cassava planting area and the continuous reduction of rural labor force, the labor cost increases rapidly, accelerating the research and development of applicable cassava harvesting machinery and improving the mechanized operation rate of cassava harvesting link have become the primary task for the research on cassava harvesting machinery in China (*Yang et al., 2024*).

Guanghao Xu, Assistant Researcher Ph.D. Eng.; Jiannong Song, Prof. Ph.D. Eng.; Zhongsheng Cao, Associate Researcher Ph.D.; Binfeng Sun, Associate Researcher Ph.D.; Junbao Huang, Assistant Researcher Ph.D.; Xinyi Peng, Assistant Researcher M.S. Eng.; Wenwen Li, M.S. Eng. Stud.; Yanda Li, Senior Researcher Ph.D.

Brazil and Thailand have higher degree of cassava mechanized harvesting. However, due to different soil conditions, cassava varieties and planting modes, the applicability of foreign cassava harvesting machinery in China remains to be studied (*Agbetoye et al., 1998; Singhpoo et al., 2023*), and there are problems such as high costs of machine transportation and later maintenance. The research on cassava harvesting machinery in China began in 2008 and is still at the primary stage of research (*Huang et al., 2012; Yang et al., 2024*). Drawing on foreign cassava harvesting machinery and through the imitation and modification of related equipment such as potato harvesters (*Awuah et al., 2023; Johnson et al., 2023; Blok et al., 2025*), Chinese researchers have developed a variety of cassava harvesters (*Liu et al., 2014; Ju et al., 2023; Yang et al., 2023*). Among these, the digging-loosening and elevating chain-type cassava harvester is currently the most widely used in China. Although this type of machinery has significantly reduced manual labor intensity, various problems encountered during its operation—such as high power consumption, excessive roots damage rate, and short service life of the chain screen—remain unresolved effectively. Consequently, the further promotion and application of cassava harvesters in China have been severely hindered.

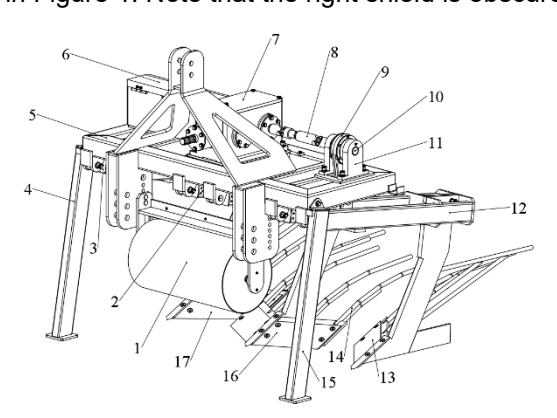
In view of the problems existing in the current cassava mechanized harvesting process in China, this paper developed a large-ridge double-row cassava planting mode through preliminary research and combined with the existing cassava planting agronomy in China, and designed a double-row vibrating cassava harvester based on this. According to the designed harvesting scheme, the structural design of key components such as special gear box, dynamic vibration device and excavator shovel assembly was completed. Through the analysis of the whole machine motion, the functional relationship between the structural parameters and the motion parameters of the harvester is established. The research results have certain practical value for realizing the whole process mechanization of cassava production.

#### **MATERIALS AND METHODS**

# Overall structure and main technical parameters

## Structure and working principle

The double-row vibrating cassava harvester adopts a left-right symmetrical structure and is mainly composed of the frame, special gearbox, dynamic vibration device, digging shovel assemblies, struts, shields, and depth-limiting device. The dynamic vibration device consists of the eccentric connecting rod assembly, bearing seat assembly, connecting rod shaft, and universal coupling. The digging shovel assembly includes three sections: the left shovel assembly, the middle shovel assembly, and the right shovel assembly. Each section is composed of two parts: the digging shovel and the pull rod. The main structure of the machine is shown in Figure 1. Note that the right shield is obscured in the design drawing of Figure 1a.





a. Design diagram

b. Physical diagram

Fig. 1 - Double-row vibrating cassava harvester

1.Depth limiting device; 2.Middle tie rod; 3.Left tie rod; 4.Left strut; 5.Frame; 6.Left shield; 7.Special gearbox; 8.Universal coupling; 9. Eccentric connecting rod assembly; 10.Connecting rod shaft; 11.Bearing seat assembly; 12.Right tie rod; 13.Right digging shovel; 14.Separation lever; 15.Right strut; 16.Middle digging shovel; 17.Left digging shovel

The double-row vibrating cassava harvester is designed to operate with a supporting tractor rated at 55.2~66.2 kW. During harvesting, the machine is mounted on the rear three-point hitch and pulled forward by the tractor. Power from the tractor's rear PTO is transmitted to the dynamic vibration device through the special gearbox after two-stage speed reduction, which then drives the digging-shovel assemblies to reciprocate about their pivot points on the frame. During operation, the depth-limiting device first breaks the surface of the cassava ridge.

Table 1

The digging shovels then penetrate beneath the cassava root-soil complex and lift it upward. Simultaneously, the reciprocating motion of the digging shovels impacts and agitates the root-soil complex, accelerating the disintegration of soil clods. As the harvester moves forward, the lifted cassava root-soil complex continues to undergo soil breakup on the separation rods welded behind the digging shovels; the loosened soil falls through the gaps between the rods, thereby completing the cassava root-soil separation process. After separation, the cassava roots are laid flat on the ground behind the machine.

## Main technical parameters

The main technical parameters of the designed double-row vibrating cassava harvester are shown in Table 1 in combination with the agronomic requirements of cassava planting and the growth characteristics of cassava roots.

Main technical parameters of double-row vibrating cassava harvester

**Project Values Boundary dimensions** 1 940×1 750×1 670 (length×width×height)/mm Total mass / kg 780 Required tractor power / kW 55.2 ~ 66.2 Rear three-point Hitch type suspension Digging depth (5-level adjustable) / mm 252 ~ 350 Effective working width / mm 1330 Pure working productivity / (hm²/h) ≥0.3 2 **Number of rows** 

# Design of supporting planting pattern

The main impacts of the existing planting methods on cassava mechanized harvesting operations are as follows: (1) most of the cassava planting areas in China are heavy soil, and because the cassava is deeply rooted and the harvest period is in the southern rainy season, the cassava planting land is seriously dry and hardened, which brings great difficulties to the harvesting machinery operations (Amponsah et al., 2014); (2) The roots and stems of cassava grown in the ground grow disorderly. When the cassava straw is crushed and returned to the field, it is difficult to distinguish the growth position of cassava on the ground, resulting in the unit being unable to go down or work in the opposite direction; (3) The current row spacing of cassava planting in ridge cultivation is not uniform, and the matching with tractor track and harvester operation width is poor, resulting in the crushing of cassava by tractor or the inability of the harvester to operate effectively.

Through literature review and field investigations, the research team developed and defined a "largeridge, double-row" cassava planting mode. The main technical points are as follows: the shape of the ridge is trapezoid, the ridge-bottom width L<sub>2</sub> is about 120 cm, the ridge-top width L<sub>3</sub> is about 90~100 cm, the height h is about 25~30 cm, and the on-ridge row spacing L4 is about 50 cm; each ridge is planted in two rows, the inter-ridge row spacing L₅ is about 60~70 cm, the distance between the rows L₆ is about 100~110 cm, and the plant distance is about 60~70 cm. When the tractor's supporting power is 55.2-66.2 kW, taking the domestic Dongfanghong LX series tractor as an example, the corresponding outer tractor wheel spacing L is less than 220 cm, the inner tractor wheel spacing L<sub>1</sub> is greater than 120 cm, and the minimum ground clearance meets the requirements of the "large-ridge, double-row" cassava planting mode. This planting mode effectively reduces the working resistance of the harvester during cassava harvesting and resolves operational issues such as the tractor's inability to travel between adjacent rows, root damage caused by wheel loading, and mismatches between tractor wheel spacing and harvester working width. The research team, in collaboration with relevant institutions, has carried out promotion trials of the "large-ridge, double-row" cassava planting mode in Guangdong, Guangxi, Hainan, and Jiangxi since 2017, achieving favorable comprehensive economic benefits (Deng et al., 2019). The structural layout of the "large-ridge, double-row" cassava planting mode is shown in Figure 2.

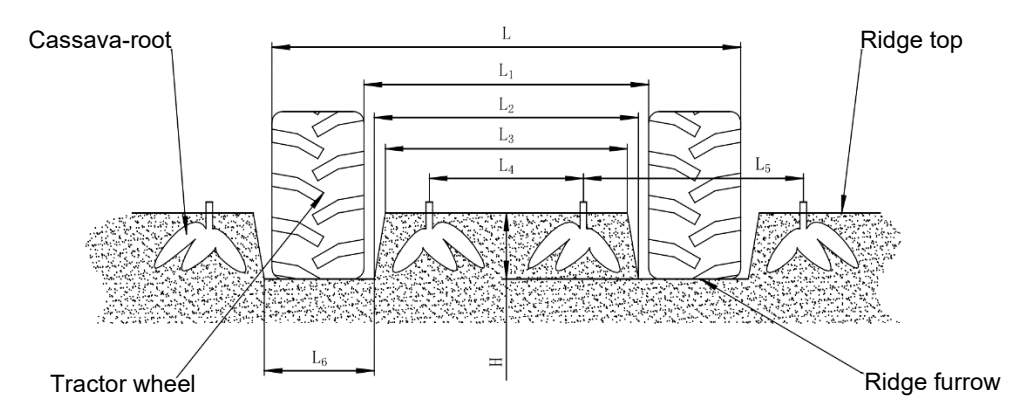


Fig. 2 - Schematic diagram of the "large-ridge, double-row" cassava planting model Note: L is the outer tractor wheel spacing, cm;  $L_1$  is the inner tractor wheel spacing, cm;  $L_2$  is the ridge-bottom width, cm;  $L_3$  is the ridge-top width, cm;  $L_4$  is the on-ridge row spacing, cm;  $L_5$  is the inter-ridge row spacing, cm;  $L_6$  is the ridge-furrow width, cm; H is the ridge height, cm.

## Structural design and parameter determination of key components of harvester Special gearbox design

The power is transmitted from the rear output shaft of the tractor to the input shaft of the special gearbox through the universal joint. After secondary deceleration, the output shaft drives the middle eccentric connecting rod assembly to rotate. At the same time, it is transmitted to the connecting rod shafts on both sides of the machine through the universal couplings on the left and right sides of the output shaft to drive the eccentric connecting rod assemblies on both sides to rotate. The power transmission route of the whole machine is shown in Figure 3.

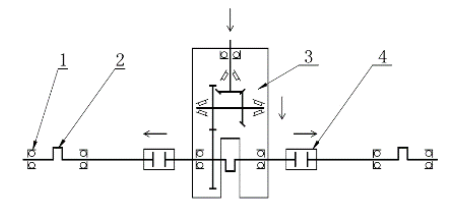


Fig. 3 - Road map of harvester power transmission

1. Bearing seat assembly; 2. Connecting rod assembly; 3. Special gearbox; 4. Universal coupling

Most existing agricultural gearboxes provide power output either from both ends or from a single end of the output shaft. To eliminate the over-constraint problem of the shovel assemblies in the harvester and to achieve a more compact overall structure, a three-output gearbox was designed. The special gearbox adopts a two-stage transmission: the first stage uses a straight bevel gear pair, and the second stage uses a straight cylindrical gear pair. The front horizontal shaft functions as the input shaft, while the rear vertical shaft serves as the output shaft. Power output terminals are arranged at the left end, right end, and center of the output shaft, as shown in Figure 4.

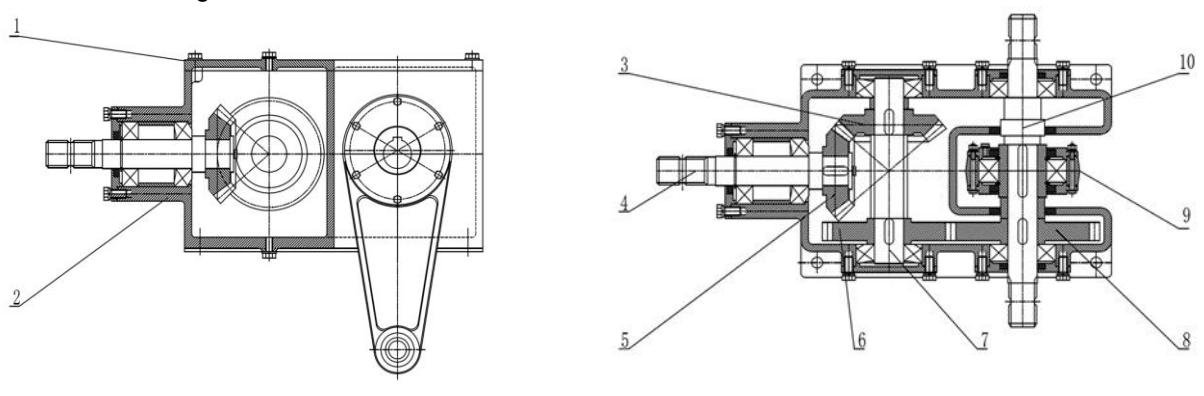


Fig. 4 - Structure diagram of special gearbox

b. Top view

a. Main view

1. Box cover; 2. Box body; 3. Large spur bevel gear; 4. Input shaft; 5. Small spur bevel gear; 6. Small spur gear; 7. Intermediate shaft; 8. Large spur gear; 9. Connecting rod assembly; 10. Output shaft

Since the output bearing carries all the torque output of the harvester, the preliminary calculation of the shaft diameter is carried out according to the torsional strength criteria. The torsional strength conditions of the transmission torque shaft are (Sun et al., 2021):

$$\tau = \frac{T}{W_T} = \frac{9.55 \times 10^6 P}{0.2d^3 n} \le [\tau] \text{ [MPa]}$$
 (1)

 $\tau = \frac{\tau}{W_T} = \frac{9.55 \times 10^6 P}{0.2 d^3 n} \leq [\tau] \text{ [MPa]}$  In equation:  $\tau$  - torsional shear stress on the shaft, [MPa];

T - shaft torque, [N·mm];

 $W_T$ - torsional section modulus of shaft, [mm<sup>3</sup>];

P - maximum power transmitted by the shaft, [kW];

d - shaft diameter, [mm];

*n* - shaft rotational speed, [r/min];

 $\tau$  - allowable shear stress of the shaft material, [MPa].

From the above formula, the diameter of the shaft is:

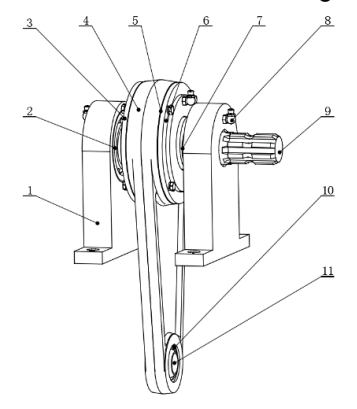
$$d \ge \sqrt[3]{\frac{9.55 \times 10^6}{0.2[\tau]} \sqrt[3]{\frac{P}{n}}} = C \sqrt[3]{\frac{P}{n}} [\text{mm}]$$
 (2)

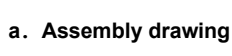
where: C - coefficient determined by the shaft material and allowable shear stress, defined as,  $C = \sqrt[3]{\frac{9.55 \times 10^6}{0.2[\tau]}}$ .

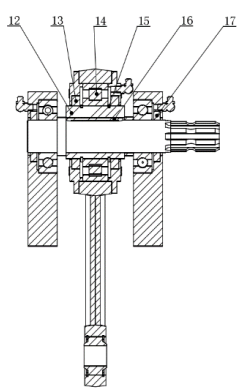
According to the "Agricultural Machinery Design Manual" and the field test of similar machinery (Sun et al., 2016), the power transmitted by the shaft is taken as p=10 kW, the output shaft speed n is about 400 r/min after two-stage deceleration, the shaft is made of 45 steel, the load on the shaft is mainly torque and the soil in cassava planting area is sticky, so C is taken as 120. By substituting the data into formula (2), it can be obtained that  $d \geq 35.09$  mm. Because there are two keyways on the shaft, the shaft diameter should be increased by  $7\sim10\%$ . Combined with the inner diameter of the bearing inner ring of the output shaft, d=40 mm.

## Structural design of dynamic vibration components

Figure 5 is the structural diagram of the dynamic vibration device, which is mainly composed of bearing seat assembly, eccentric connecting rod assembly, connecting rod shaft and universal coupling. The bearing seat assembly is composed of a bearing seat, a single side sealed deep groove ball bearing, a sealing ring and a right angle grease fitting. The eccentric connecting rod assembly is mainly composed of connecting rod, left (right) end cap, eccentric shaft sleeve, NUP cylindrical roller bearing and spherical plain bearing. The two bearing seat assemblies are symmetrically installed. The eccentric connecting rod assembly is supported by the connecting rod shaft, and the articulated bearing at the lower end is connected with the pull rod pin seat through the connecting rod pin shaft. Since the dynamic vibration device is subjected to substantial vibration and impact loads, and considering both the speed factor (dn, where d is the inner diameter of the rolling bearing, mm; n is the bearing rotational speed, r/min) and the circumferential speed of the shaft (Sun et al., 2021), the bearings in the bearing-seat assembly and the eccentric connecting-rod assembly are designed with contact-type seals and lubricated with grease.







b. Half section

Fig. 5 - Structure diagram of power vibration components

Bearing seat 2. Single-side-sealed deep-groove ball bearing 3. Left end cover 4. Connecting rod 5. Paper pad 6. Right end cover 7.
 Connecting-rod shaft spacer 8. Grease nipple 9. Connecting-rod shaft 10. Circlip for hole 11. Joint bearing 12. Eccentric shaft sleeve 13.
 Connecting rod sealing ring 14. NUP cylindrical roller bearing 15. Circlip for shaft 16. Flat key 17. Bearing seat sealing ring

The severe vibration during the harvesting operation of three groups of shovels of cassava harvester will reduce the service life of the whole machine. According to the relevant literature research, the adverse impact of vibration on the machine can be greatly reduced by adopting the "small amplitude, large vibration frequency" motion of the vibrating parts combined with the self-balancing relationship between multiple groups of shovels in the process of vibration utilization. Based on the previous research results and considering the spatial size of the dynamic vibration device (*Sun et al., 2016*), the eccentricity of the eccentric shaft sleeve is designed to be 5 mm, the center distance of the connecting rod is 275 mm, and the diameter of the connecting rod shaft is the same as that of the rear output shaft of the gearbox, which is 40 mm.

# Design and motion analysis of excavator shovel assembly Structure design and key parameters of excavator shovel assembly

The digging shovel is the key component that directly affects the operation quality of the rhizome harvester. Because cassava roots grow deep in the soil and the digging resistance is high during harvesting, the digging shovel must have a simple structure and operate reliably. The excavator shovel assembly of this machine consists of three units: the left shovel assembly, the right shovel assembly, and the middle shovel assembly. Each assembly contains two components - the digging shovel and the pull rod. The digging shovel is mounted on the shovel-mounting seat located behind the pull rod and is secured with bolts and nuts. The pull rod is connected to the frame and to the eccentric connecting-rod assembly through the pull-rod pin shaft and the connecting-rod pin shaft, respectively. Each digging shovel is mainly composed of a shovel seat, shovel surface, and shovel tip. The shovel seat is a welded component formed by joining the shovel handle, base, support plate, separation rod, reinforcing plate, and the side plate (the side plate is unique to the left and right shovel seats). The primary soil-engaging parts - the shovel tip and shovel surface - are replaceable components made of high-quality carbon steel with good hardenability and subjected to overall quenching treatment. The upper surfaces of all cutting edges are overlaid with wear-resistant electrode material to enhance the working performance and service life of the digging shovels. The structure of the digging shovel assembly is shown in Figure 6.

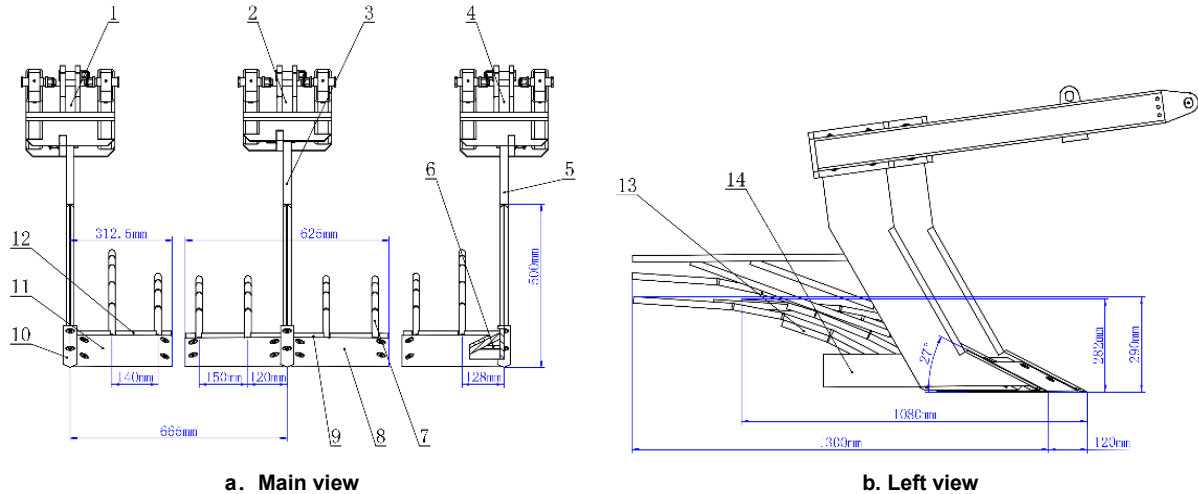


Fig. 6 - Assembly structure diagram of the excavating shovel
1. Left lever; 2. Middle lever; 3. Middle shovel handle; 4. Right lever; 5. Side shovel handle; 6. Support plate;
7. Separation rod; 8. Middle shovel surface; 9. Middle base; 10. Shovel tip; 11. Side shovel surface;
12. Side base; 13. Strengthening rod; 14. Side panel

The middle shovel adopts a double-wing symmetrical structure, while the left and right digging shovels are single-wing structures arranged symmetrically to each other. The specific structure and main working parameters are shown in Figure 6. To prevent the shovel handle from cutting or damaging the cassava roots, the handle is designed with a broken-line profile, ensuring that the bottom of the digging shovel enters beneath the cassava roots first. This allows the cassava root-soil complex to move into the space between the middle shovel and the left (or right) shovel. The middle digging shovel operates slightly ahead of the left and right shovels, and its horizontal excavation and screening distance is slightly shorter than that of the side shovels. This arrangement enables the two rows of cassava roots to converge behind the middle shovel after excavation, thereby preventing the tractor wheels from pressing on the harvested cassava roots when the machine proceeds to the adjacent ridge.

According to the ridge-shape parameters of the "large-ridge, double-row" cultivation mode and the planting row spacing of cassava on the ridge, combined with the root-growth characteristics of cassava and verified through preliminary prototype tests, the following structural parameters were determined: the digging-shovel penetration angle is 27°; the spacing between the middle digging shovel and the left (right) digging shovel is 665 mm; the effective working width is 1330 mm; and the horizontal distance between the middle shovel tip and the left (right) shovel tip is 120 mm. The middle digging shovel has a horizontal wingspan of 625 mm, a digging-and-screening horizontal distance of 1080 mm, and a vertical height of 282 mm. The left (right) digging shovel has a horizontal wingspan of 312.5 mm, a digging-and-screening horizontal distance of 1300 mm, and a vertical height of 290 mm.

## **Analysis of motion characteristics**

The soil disturbance generated by different motion patterns of the digging shovel during harvesting directly affects the operational performance of the harvester. To analyze the shovel's behavior in the soil, the motion characteristics of the digging shovel were examined using the middle shovel assembly as a representative example.

The front end of the pull rod of the middle shovel assembly is connected to the frame through the pull-rod pin shaft, while the middle and upper sections of the pull rod are connected to the lower end of the eccentric connecting-rod assembly through the connecting-rod pin shaft. Driven by the eccentric connecting-rod assembly, the middle shovel assembly oscillates at a small angle about its mounting point on the frame, and its motion can be simplified as that of a crank-rocker mechanism. A fixed coordinate system xOy is established with the center of the cylindrical surface of the pull-rod pin shaft on the frame as the origin O. The horizontal direction is taken as the x-axis (positive to the right), and the vertical direction as the y-axis (positive upward). A dynamic coordinate system  $x_1O_1y_1$  is established with the center of the cylindrical surface of the gearbox output shaft as the origin  $O_1$ ; the line  $O_1O$  serves as the horizontal axis, and the vertical line through  $O_1$  serves as the vertical axis. The positive orientations of the axes in the dynamic coordinate system are shown in Figure 7. The projections of the moving-system origin  $O_1$  onto the x- and y-axes of the fixed coordinate system are denoted  $x_{O_1}$  and  $y_{O_1}$ , respectively. Point A is the center of the cylindrical surface of the eccentric-shaft sleeve, point B is the center of the cylindrical surface of the connecting-rod pin shaft,  $O_2$  is the tip of the middle digging shovel,  $C_1$  is the perpendicular projection of  $O_2$  onto the  $y_1$ -axis.

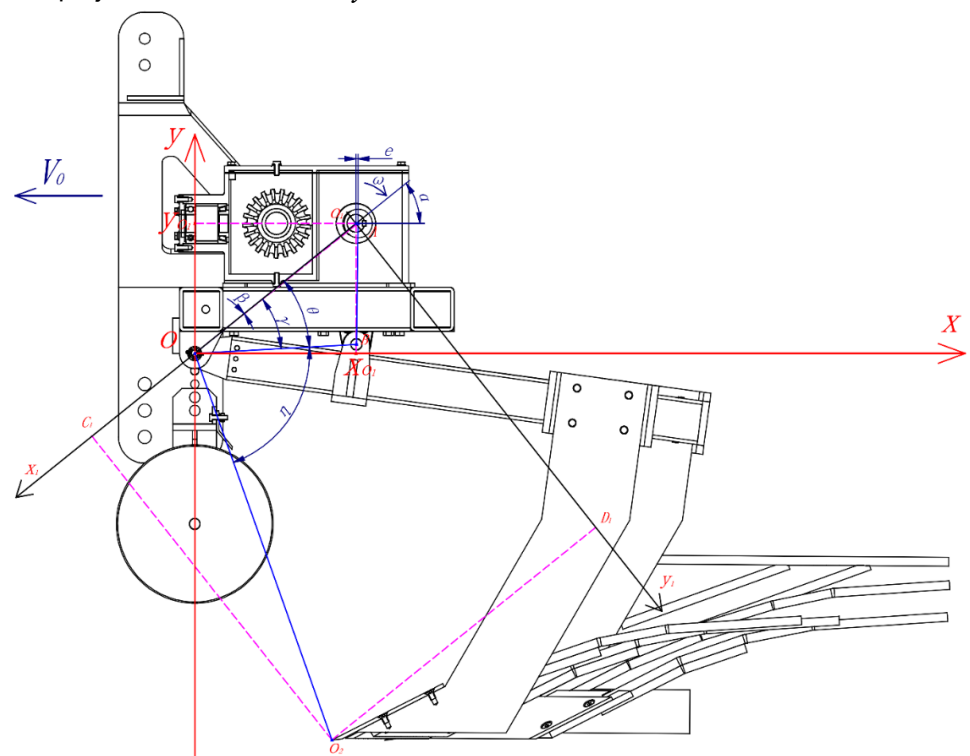


Fig. 7 - Motion analysis diagram of the middle excavating shovel

In the "crank rocker mechanism",  $O_1A$  is the "crank", that is, the eccentricity of the eccentric shaft sleeve e, AB is the "connecting rod", that is, the center distance of the connecting rod in the machine  $L_{AB}$ , OB is the "rocker", that is, the center of the cylindrical surface of the pull rod pin shaft to the center of the cylindrical surface of the connecting rod pin shaft  $L_{OB}$ ,  $OO_1$  is the "fixed frame", that is, the center distance from the cylindrical surface center of the pull rod pin shaft to the center point of the gearbox output shaft  $L_{OO_1}$ . The included angle between the crank  $O_1A$  and the  $x_1$  axis of the dynamic coordinate system (fixed frame  $OO_1$ ) is  $\alpha$ . For the convenience of calculation, the initial position of the crank  $O_1A$  is parallel to the x axis of the fixed coordinate system, and the initial value of the angle  $\alpha$  is  $\alpha_0$ ; The included angle between the rocker OB and the  $x_1$  axis of the moving coordinate system is  $\theta$ , the included angle with  $OO_2$  is a fixed value, and the size is  $\eta$ ; connecting point A and point A0, the distance between AO0 is A1 included angle between AO2 and the A2 axis of the moving coordinate system is A3, and the included angle with rocker A4 is A5, connecting point A5 and the A6 distance between A7 and the included angle between A8 is A9, connecting point A9 and the A9 is the distance between A9 is the angular velocity of crank A9, and the rotation direction is clockwise; A9 is the forward speed of the harvester, and the forward direction is horizontally left.

As shown in Figure 8, the "crank rocker mechanism" of the machine is separated from the dynamic coordinate system  $x_iO_iy_i$ , and its motion is analyzed using the analytical method (*Qin et al., 2019*):

(1) Angular displacement analysis

The angular displacement of crank  $O_IA$  is:

$$\alpha = \alpha_0 + \omega \cdot t \text{ [rad]} \tag{3}$$

In equation:

 $\alpha$  - angle between crank  $O_IA$  and  $x_I$  axis of dynamic coordinate system, [rad];

 $\alpha_0$ - initial value of angle  $\alpha$ , [rad];

 $\omega$  - angular velocity of crank  $O_1A$ , [rad/s];

t - time, [s].

In triangle  $O_1AO$ , the sine theorem can be used to obtain:

$$\beta = \tan^{-1} \frac{e \cdot \sin \alpha}{l_{OO_1}} [\text{rad}] \tag{4}$$

In equation:

 $\beta$  - angle between crank AO and  $x_I$  axis of dynamic coordinate system, [rad];

 $\omega$  - length of crank  $O_IA$ , [mm];

 $l_{OO_1}$  - length of fixed frame  $OO_I$ , [mm].

In triangle  $O_lAO$ , the cosine theorem can be used to obtain:

$$l_{AO}^2 = e^2 + l_{OO_1}^2 + 2el_{OO_1} \cos \alpha \text{ [mm]}$$
 (5)

In equation:

 $l_{AO}$  - distance between point A and point O, [mm].

In triangle AOB, the cosine theorem can be used to obtain:

$$\gamma = \cos^{-1} \frac{e^2 + l_{OO_1}^2 + l_{OB}^2 - l_{AB}^2 + 2el_{OO_1} \cos \alpha}{2l_{AO}l_{DB}}$$
[rad] (6)

In equation:

 $\gamma$  - angle between connecting line AO and rocker OB, [rad];

 $l_{OB}$  - length of rocker OB, [mm];

 $l_{AB}$  - Length of connecting rod AB, [mm].

From above equations, the angular displacement equation of rocker OB is:

$$\theta = \beta + \gamma \text{ [rad]} \tag{7}$$

In equation:  $\beta$  - included angle between rocker OB and fixed frame  $OO_I$ , [rad].

The angular displacement equation of line  $OO_2$  is:

$$\delta = \theta + \eta \text{ [rad]} \tag{8}$$

In equation:

 $\beta$  - included angle between line  $OO_2$  and fixed frame  $OO_1$ , [rad];

 $\eta$  - included angle between rocker OB and line  $OO_2$ , [rad].

By substituting equation (4), equation (6) and equation (7) into equation (8) the final angular-displacement equation of line  $OO_2$  is obtained as follows:

$$\delta = \tan^{-1} \frac{e \cdot \sin \alpha}{l_{OO_1}} + \cos^{-1} \frac{e^2 + l_{OO_1}^2 + l_{OB}^2 - l_{AB}^2 + 2e l_{OO_1} \cos \alpha}{2l_{AO} l_{OB}} + \eta \text{ [rad]}$$
(9)

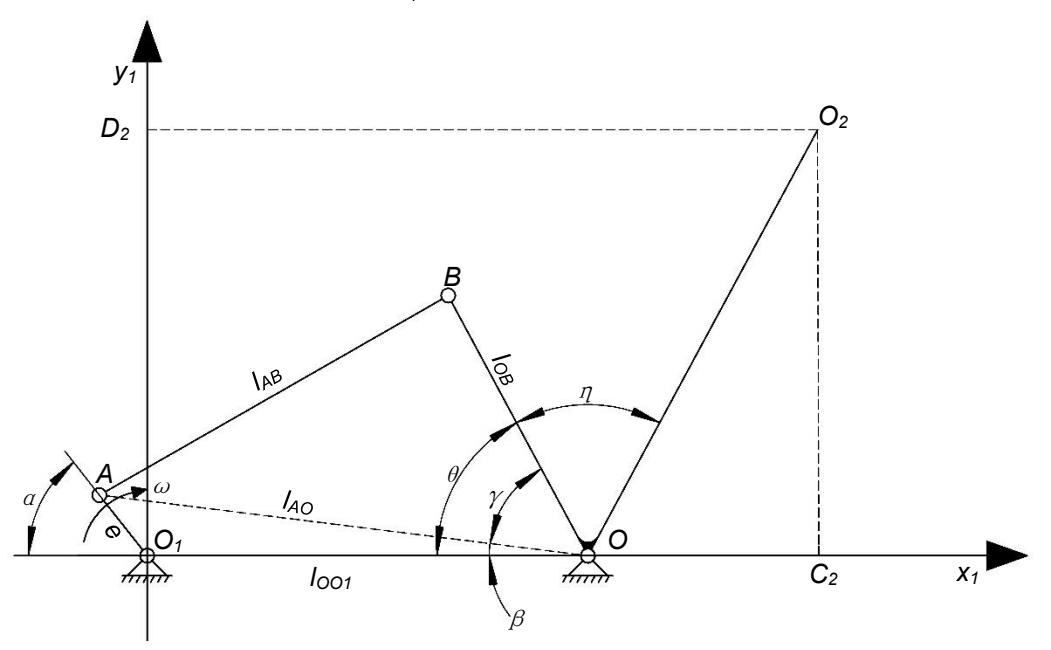


Fig. 8 - Schematic diagram of crank rocker mechanism and dynamic coordinate system

### (2) Analysis of shovel tip trajectory

The relative trajectory equation of point  $O_2$  in the moving coordinate system  $x_1O_1y_1$  is:

$$\begin{cases} x_{C_1} = l_{0O_1} - l_{0O_2} \cdot \cos \delta \\ y_{D_1} = l_{0O_2} \cdot \sin \delta \end{cases}$$
 (10)

In equation:

 $l_{00_2}$  - Distance between point O and point  $O_2$ , [mm].

The motion of the moving coordinate system  $x_lO_ly_l$  relative to the fixed coordinate system xOy can be fully described by the following three equations:

$$\begin{cases} x_{O_1} = X_{O_1} - V_0 \cdot t \\ y_{O_1} = Y_{O_1} \\ \varphi = \pi + \alpha_0 \end{cases}$$
 (11)

In equation:

 $V_0$  - forward speed of harvester, [mm/s];

 $X_{O_1}$ - initial abscissa of point  $O_I$  in the fixed coordinate system xOy, [mm];

 $Y_{O_1}$  - Initial ordinate of point  $O_I$  in the fixed coordinate system xOy, [mm];

 $\varphi$  - the rotation angle from the horizontal axis of the fixed coordinate system xOy to the horizontal axis of the moving coordinate system  $x_IO_Iy_I$  is positive in the counterclockwise direction, [rad].

The coordinate transformation relationship between the moving coordinate system  $x_iO_iy_i$  and the fixed coordinate system xOy is (Harbin Institute of Technology Theoretical Mechanics Teaching and Research Section, 2023):

$$\begin{cases} x = x_{O_1} + x_{C_1} \cdot \cos \varphi - y_{D_1} \cdot \sin \varphi \\ y = y_{O_1} + x_{C_1} \cdot \sin \varphi + y_{D_1} \cdot \cos \varphi \end{cases}$$
 (12)

Using the coordinate transformation relationship between the moving coordinate system  $x_1O_1y_1$  and the fixed coordinate system xOy, the relative motion trajectory equation formula (10) of point  $O_2$  in the moving coordinate system  $x_1O_1y_1$  is substituted into formula (12), and the absolute motion trajectory equation of point  $O_2$  can be obtained as follows:

$$\begin{cases} x = X_{O_1} - l_{OO_1} \cdot \cos \alpha_0 - V_0 \cdot t + l_{OO_2} \cdot \cos(\delta - \alpha_0) \\ y = Y_{O_1} - l_{OO_1} \cdot \sin \alpha_0 - l_{OO_2} \cdot \sin(\delta - \alpha_0) \end{cases}$$
(13)

When the forward speed  $V_{\theta}$  and the rear output shaft speed  $\omega$  of the gearbox are given, it can be seen from formula (9) that angle  $\delta$  is a variable related to time t, that is, there is only a unique variable time t in formula (13). When the forward speed  $V_{\theta}$  of the harvester is given to be 1000 mm/s, the rear output shaft speed of the special gearbox is  $\omega=13.22$  rad/s (the corresponding rear output shaft speed of the tractor is 540 r/min), and the motion time is t=0.5 s, the absolute motion trajectory of the shovel tip  $O_2$  point in the fixed coordinate system xOy can be obtained through MATLAB software programming, which is similar to a wave shape (Shahgoli et al., 2009; Shahgoli et al., 2010). The curve is shown in Figure 9.

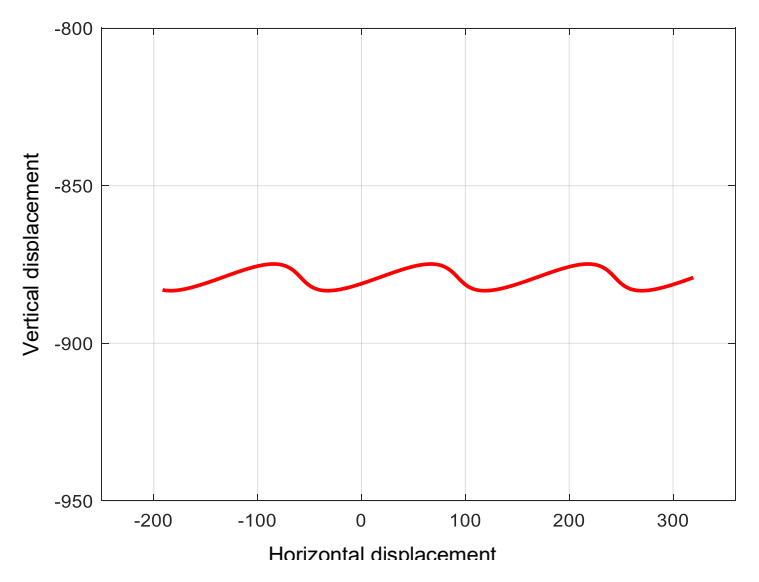


Fig. 9 - Absolute trajectory of the shovel tip  $O_2$  in the fixed coordinate system xOy

It can be seen from the movement track shown in Figure 9 that the working process of the shovel assembly in the soil includes three stages: cutting the soil, throwing up the cassava roots-soil complex and impacting cassava roots-soil complex. The throwing up and impact process of the digging shovel on the cassava roots-soil complex plays an important role for the crushing of soil in the cassava roots-soil complex. Therefore, in order to ensure the separation effect of cassava roots and soil during the operation of the harvester, it is necessary to make the shovel component throw and impact the cassava roots-soil complex for a certain number of times within the forward unit distance of the harvester. According to the swing law of the excavator shovel assembly, the harvester advances a certain distance, that is, the ridge of unit length. The impact times of the excavator shovel on the ridge are:

$$\lambda = \frac{L_0 \cdot \omega}{2\pi \cdot V_0} \tag{14}$$

In the equation:  $\lambda$  - impact times of digging shovel on ridge per unit length;  $L_0$ - ridge distance per unit length, [mm].

According to the research results of literature [30], the existing tractor rear output shaft speed is mostly adjustable by two parties. The design values of gearbox rear output shaft speed (crank  $O_1A$  angular speed)  $\omega$  are 13.22  $\pi$  and 17.64  $\pi$  rad/s, and the corresponding excavator vibration frequencies are 6.61 and 8.82 Hz respectively. The reasonable ratio between harvester forward speed  $V_0$  and gearbox rear output shaft two speeds  $\omega$  can be determined through field test.

#### **RESULTS**

## Field test conditions

After the prototype of the double-row vibrating cassava harvester was manufactured, the research team conducted a field harvest performance test of the prototype in the cassava production mechanization test demonstration base of the Institute of Agricultural Machinery, Chinese Academy of Tropical Agricultural Sciences, Zhanjiang, Guangdong Province. The planting mode of cassava in the experimental plot was "largeridge and double-rows" planting mode, and the variety was "Nanzhi 199", with a planting area of about 2 hm²; Before the experiment, the average ridge spacing was 1655 mm, the plant spacing on the ridge was 650 mm, the row spacing was 600 mm, and the cassava roots setting depth was 220~300 mm; the soil type was latosol, the soil moisture content was 15.9~19.9%, and the soil firmness was 1.86~3.02 MPa. The tractor brand and model for the harvester test was Dongfanghong LX-904, with a power of 66.2 kW, the rear output shaft speed of 540/720 r/min, two gears were adjustable, and the track width and ground clearance met the operation requirements. One or two days before harvest, the cassava stalks in the test site were mechanically crushed and returned to the field. After treatment, there was no vertical cassava stalk residue on the top surface of the ridge. Killing seedlings in advance and drying the plot reduced the soil moisture content, which was conducive to the separation of cassava root and soil during harvest. The field operating conditions of the test site and the performance of the prototype after the pre-harvest mechanical straw crushing treatment are shown in Fig.10.



a. Test site



c. Field trial



b. Field commissioning



d. Operation effect

Fig. 10 - Test site and prototype field test

## Test plan and results

## **Determination of test parameters**

Before the test, through trial excavation, the damage of cassava roots excavated by the harvester at different gears of the depth limiting wheel was compared. Cassava roots were occasionally cut off by the digging shovel at the first gear depth (252 mm), while cassava roots were not cut off by the digging shovel at the second gear depth (282 mm) and the third gear depth (312 mm). In this experiment, the excavation depth of the second gear was selected, that is, the excavation depth was 282 mm. The working conditions of the tractor and the harvester were compared when the rear output shaft speed of the tractor was 540 r/min and 720 r/min. It was found that when the speed was 720 r/min, although the soil crushing effect was increased, the degree of cassava root buried by the soil crushing was also increased, and the operating noise and vibration amplitude of the harvester were significantly increased. Therefore, after this test, the output shaft speed was 540 r/min, and the vibration frequency of the excavator was about 6.61 Hz.

After adjusting the gear of the depth limiting wheel and the rear output shaft speed of the tractor, the tractor pulled the harvester through the three-point suspension for field test.

According to the test procedures and relevant mechanical test methods specified in the national industry standard for potato harvesters (*Wei et al., 2023; Lv et al., 2024*), *Technical Specification for Quality Evaluation of Potato Harvesters* (NY/T 648-2002), each measurement section in this test was set to a length of 20 m. A 10 m preparatory section was arranged before each measurement section to allow for fine adjustment of the operating state of the tractor and harvester, ensuring that both machines reached a stable working condition before entering the measurement area. The test mainly measured the performance of four working performance indexes of the harvester, including total loss rate, clean cassava roots rate, damaged cassava roots rate and pure working-hour productivity, when the rear output shaft speed of the tractor was 540 r/min, in two different forward gears of "low-speed third gear" and "medium-speed first gear" (each gear tested twice). During each trial, the travel time through the measuring area was recorded separately. After the operation, the harvested cassava tubers from each test area were collected, classified, and weighed for data recording.

#### **Test results**

The test results of this field test are shown in Table 2.

Table 2
Test results of the main working performance indexes of the prototype at different forward speeds

Performance indicators	Design requirements	Forward gear			
		Low-speed third gear		Medium-speed first gear	
Total loss rate/%	≤5	4.05	1.29	0.65	1.99
Clean cassava roots rate /%	≥95	95.95	98.71	99.35	98.01
Damaged cassava roots rate /%	≤5	1.77	1.08	0.93	1.30
Pure working hour productivity /(hm²/h)	≥0.30	0.52	0.52	0.65	0.65

During the tests, the unit exhibited good mobility and no noticeable vibration transfer to the tractor. All components of the harvester operated smoothly and reliably, soil flow during the harvesting process was unobstructed, and the cassava root-soil separation performance was satisfactory. When the tractor rear PTO speed was 540 r/min (corresponding to a digging-shovel vibration frequency of 6.61 Hz) and the forward speeds were 0.87 m/s and 1.10 m/s, the prototype achieved average pure working productivities of 0.52 hm²/h and 0.65 hm²/h, respectively. The average clean-root rates were 97.33% and 98.68%, the average damaged-root rates were 1.43% and 1.12%, and the average total loss rates were 2.67% and 1.32%, respectively. Therefore, under optimal operating conditions, the recommended forward speed of the harvester is  $V_0$ =1.10m/s, with a rear PTO speed of  $\omega$ =540r/min.

#### **CONCLUSIONS**

- (1) The research team developed the "large-ridge, double-row" cassava planting mode.
- (2) Based on this planting mode, a double-row vibrating cassava harvester was designed. The structures of the key operating components including the special gearbox, dynamic vibration device, and digging-shovel assemblies were designed, and the overall machine parameters were determined. The harvester completes, in a single operation, the excavation and conveyance of two rows of cassava, cassava root-soil separation, and the final laying of cassava roots. The machine features a simple and compact structure. The tractor rear PTO provides the driving torque for the power vibration device, which alternately drives the three digging shovels to vibrate during operation. This improves cassava root-soil separation, reduces digging resistance, and enables self-balancing of the harvester, significantly decreasing vibration transmission to the tractor via the rear suspension.
- (2) Taking the motion of the shovel tip of the middle shovel assembly as an example, the functional relationship between structural parameters and motion parameters was established using analytical methods. MATLAB was used to obtain the absolute motion trajectory of the shovel tip. Combined with this trajectory, the micro-movement process of the digging shovel in the soil was analyzed, providing a theoretical basis for the future optimization of structural and operational parameters of the machine.

(3) Field tests showed that under optimal operating conditions, the clean-root rate reached 99.35%, the damaged-root rate was 0.93%, the total loss rate was 0.65%, and the pure working productivity was 0.65  $\,$  hm<sup>2</sup>/h. All operational performance indicators meet the relevant requirements, and the machine achieved the intended design objectives.

#### **ACKNOWLEDGEMENT**

This work was supported by Jiangxi Provincial Natural Science Foundation, Research on the low loss and efficient mining and separation mechanism of cassava based on the coupling effect of forced vibration and gradual throwing, project number 20232BAB215029.

### **REFERENCES**

- [1] Agbetoye, L. A. S., Kilgour, J., & Dyson, J. (1998). Performance evaluation of three pre-lift soil loosening devices for cassava root harvesting. *Soil and Tillage Research*, 48(4), 297-302. https://doi.org/10.1016/S0167-1987(98)00136-6
- [2] Amponsah, S. K., Bobobee, E. Y. H., Agyare, W. A., Okyere, J. B., Aveyire, J., King, S. R., & Sarkodie-A. J. (2014). Mechanical cassava harvesting as influenced by seedbed preparation and cassava variety. *Applied Engineering in Agriculture*, 30(3), 391-403. <a href="https://doi.org/10.13031/aea.30.10495">https://doi.org/10.13031/aea.30.10495</a>
- [3] Awuah, E., Aikins, K. A., Antille, D. L., Zhou, J., Gbenontin, B. V., Mecha, P., & Liang, Z. (2023). Discrete Element Method Simulation and Field Evaluation of a Vibrating Root-Tuber Shovel in Cohesive and Frictional Soils. *Agriculture*, 13(8), 1525. https://doi.org/10.3390/agriculture13081525
- [4] Blok, P. M., Magistri, F., Stachniss, C., Wang, H., Burridge, J., & Guo, W. (2025). High-throughput 3D shape completion of potato tubers on a harvester. *Computers and Electronics in Agriculture*, 2025 (228), 109673. https://doi.org/10.1016/j.compag.2024.109673
- [5] Deng G., He X., Lv Y., Zheng S., Cui Z., Qin S., & He F. (2019). Study on wide and narrow double-row ridging cultivation mode and mechanized planting of cassava (木薯宽窄双行起垄栽培模式及机械化种植技术 研 究 ). *Guangdong Agricultural Sciences*, 46(5), 142-148. https://doi.org/10.16768/j.issn.1004-874X.2019.05.020
- [6] Ferraro V., Piccirillo C., Tomlins K., & Pintado M.E. (2016). Cassava (manihot esculenta crantz) and yam (dioscorea spp.) crops and their derived foodstuffs: safety, security and nutritional value. *Critical Reviews in Food Science and Nutrition*, 56(16), 2714-2727. https://doi.org/10.1080/10408398.2014.922045
- [7] Huang H., Cui Z., Zhang Y., & Xue Z. (2012). Research progress and analysis of cassava harvester (木 薯 收 获 机 械 研 究 进 展 与 分 析 ). *China Tropical Agriculture*, 2012(6), 20-22. https://doi.org/10.3969/j.issn.1673-0658.2012.06.011
- [8] He R., Fu N., Chen H., Ye J., Chen L., Pu Y., & Zhang W. (2020). Comparison of the structural characteristics and physicochemical properties of starches from sixteen cassava germplasms cultivated in China. *International Journal of Food Properties*, 23(1), 693-707. https://doi.org/10.1080/10942912.2020.1752714
- [9] Harbin Institute of Technology Theoretical Mechanics Teaching and Research Section. (2023). Theoretical mechanics 9th Edition (理论力学, 第九版). *Higher Education Press*, Beijing, China.
- [10] Johnson, C.M., & Cheein, F.A. (2023). Machinery for potato harvesting: a state-of-the-art review. Frontiers in Plant Science, 2023(14), 1156734. https://doi.org/10.3389/fpls.2023.1156734
- [11] Ju, Y., Sun, W., Zhao, Z., Wang, H., Liu, X., Zhang, H., Li, H., & Simionescu, P. A. (2023). Development and testing of a self-propelled machine for combined potato harvesting and residual plastic film retrieval. *Machines*, 11(4), 432. https://doi.org/10.3390/machines11040432
- [12] Liu S., Weng S., Liao Y., & Zhu D. (2014). Structural bionic design for digging shovel of cassava harvester considering soil mechanics. *Applied Bionics and Biomechanics*, 11(1-2), 1-11. https://doi.org/10.3233/ABB-140089
- [13] Lv J., Liu J., Zhu X., Li J., & Qi Y. (2024). Design and experiment of potato harvester excavation device under sticky and heavy black soil conditions (黏重黑土条件下马铃薯收获机挖掘装置设计与试验). *Journal of Northeast Agricultural University*, 55(5), 76-89. https://doi.org/10.19720/j.cnki.issn.1005-9369.2024.05.008

- [14] Otun S., Escrich A., Achilonu I., Rauwane M., Lerma-Escalera J.A., Morones-Ramírez J.R., & Ríos-Solís L. (2023). The future of cassava in the era of biotechnology in Southern Africa. *Critical Reviews in Biotechnology*, 43(4), 594-612. https://doi.org/10.1080/07388551.2022.2048791
- [15] Qin D., & Xie L. (2019). Modern handbook of mechanical design 2nd edition (现代机械设计手册, 第二版). *Chemical Industry Press*, Beijing, China.
- [16] Shahgoli, G., Saunders, C., Desbiolles, J., & Fielke, J. (2009). The effect of oscillation angle on the performance of oscillatory tillage. *Soil & Tillage Research*, 104(1), 97-105. https://doi.org/10.1016/j.still.2009.01.003
- [17] Shahgoli, G., Fielke, J., Desbiolles, J., & Saunders, C. (2010). Optimising oscillation frequency in oscillatory tillage. *Soil & Tillage Research*, 106(2), 202-210. https://doi.org/10.1016/j.still.2009.10.005
- [18] Sun Y., Dong X., Song J., Liu C., Wang J., & Zhang C. (2016). Parameter optimization of vibration subsoiler test bed for reducing resistance and vibration (振动深松试验台作业参数减阻减振优化). *Transactions of the Chinese Society of Agricultural Engineering*, 32(24), 43-49. https://doi.org/10.11975/j.issn.1002-6819.2016.24.006
- [19] Sun H., Chen Z., & Ge W. (2021). Mechanical principles 9th edition (机械原理, 第九版). *Higher Education Press*, Beijing, China.
- [20] Singhpoo, T., Saengprachatanarug, K., Wongpichet, S., Posom, J., & Saikaew, K.R. (2023). Cassava stalk detection for a cassava harvesting robot based on YOLO v4 and Mask R-CNN. *Journal of Agricultural Engineering*, 54(2),2023. https://doi.org/10.4081/jae.2023.1301
- [21] Tan Y., Li C., & Zeng H. (2018). Analysis on the development of cassava production and trade in China (中国木薯生产和贸易发展分析). *World Agriculture*, 2018(10), 163-168. https://doi.org/10.13856/j.cn11-1097/s.2018.10.024
- [22] Wei z., Han M., Su G., Zhang H., Li X., & Jin C. (2023). Design and experiment of a bagging and unloading potato combine harvester (装包卸包型马铃薯联合收获机设计与试验). *Transactions of the Chinese Society for Agricultural Machinery*, 54(10), 92-104. https://doi.org/10.6041/j.issn.1000-1298.2023.10.008
- [23] Yang W., Xi J., Wang Z., Lu Z., Zheng X., Zhang D., & Huang Y. (2023). Embedded field stalk detection algorithm for digging-pulling cassava harvester Intelligent clamping and pulling device. *Agriculture*, 13(11),2144. https://doi.org/10.3390/agriculture13112144
- [24] Yang R., Zhou G., Chen D., Wang T., Lv D., & Zha X. (2024). Design and experiment of drag reduction characteristics of cassava bionic digging shovel based on red soil. *INMATEH Agricultural Engineering*, 74(3), 625-641. https://doi.org/10.35633/inmateh-74-56
- [25] Yang W., Wan X., Xi J., Zhang D., Huang Y., Zheng X., Lu Z., Deng G., & Cui Z. (2024). Study on two-sided loosening shovel of digging-pulling cassava harvester. *INMATEH Agricultural Engineering*, 74(3), 69-80. https://doi.org/10.35633/inmateh-74-06